

Nisha Singh,^a Amy C. Halliday,^a
 Matthew Knight,^a Nathan A.
 Lack,^b Edward Lowe^c and
 Grant C. Churchill^{a*}

^aDepartment of Pharmacology, University of Oxford, Mansfield Road, Oxford OX1 3QT, England, ^bKoç University School of Medicine, Rumelifeneri Yolu, Sarıyer, Istanbul, Turkey, and ^cBiochemistry Department, University of Oxford, Oxford OX1 3QU, England

Correspondence e-mail:
 grant.churchill@pharm.ox.ac.uk

Received 2 May 2012
 Accepted 8 August 2012

PDB References: *HsIMPase* 1, 4as4; *MmIMPase* 1, 4as5

Cloning, expression, purification, crystallization and X-ray analysis of inositol monophosphatase from *Mus musculus* and *Homo sapiens*

Inositol monophosphatase (IMPase) catalyses the hydrolysis of inositol monophosphate to inositol and is crucial in the phosphatidylinositol (PI) signalling pathway. Lithium, which is the drug of choice for bipolar disorder, inhibits IMPase at therapeutically relevant plasma concentrations. Both mouse IMPase 1 (*MmIMPase* 1) and human IMPase 1 (*HsIMPase* 1) were cloned into pRSET5a, expressed in *Escherichia coli*, purified and crystallized using the sitting-drop method. The structures were solved at resolutions of 2.4 and 1.7 Å, respectively. Comparison of *MmIMPase* 1 and *HsIMPase* 1 revealed a core r.m.s. deviation of 0.516 Å.

1. Introduction

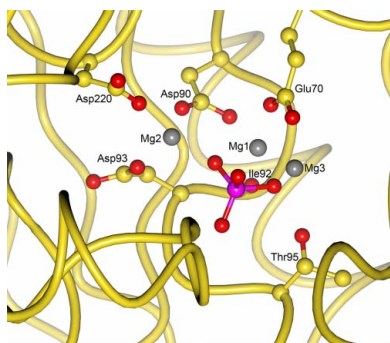
Inositol monophosphatase (IMPase) is a soluble cytosolic enzyme that catalyses the hydrolysis of inositol monophosphate (IP₁) to inositol in the phosphatidylinositol (PI) signalling cascade. Stimulation of the G_q-coupled receptor by an agonist results in the hydrolysis of phosphatidylinositol 4,5-bisphosphate (PIP₂) to diacylglycerol (DAG) and inositol (1,4,5)-trisphosphate (IP₃) by phospholipase C (PLC) (Berridge & Irvine, 1984). The inositol in IP₃ is recycled back into PIP₂ through a series of dephosphorylation steps, one of which is the dephosphorylation of IP₁ to inositol catalysed by IMPase. IMPase is also involved in the *de novo* synthesis of inositol: glucose 6-phosphate is converted to IP₁, which is then converted to inositol by IMPase. Hence, IMPase is a crucial enzyme in the PI cycle, regulating the availability of PIP₂ by controlling both the recycling and the synthesis of inositol.

IMPase is a highly conserved enzyme that is found in species as diverse as archaeobacteria (Chen & Roberts, 1998), plants (Gillaspy *et al.*, 1995) and mammals (Hallcher & Sherman, 1980; Takimoto *et al.*, 1985; Gee *et al.*, 1988). The enzyme assembles as a homodimer and requires the presence of magnesium for catalytic activity, although it is inhibited by high concentrations of magnesium and calcium and by lithium (Hallcher & Sherman, 1980), which is of therapeutic significance in bipolar disorder.

Bipolar disorder is a debilitating mental disease and the drug of choice for treatment of bipolar disorder is lithium, which inhibits IMPase at therapeutic concentrations (Hallcher & Sherman, 1980).

Crystal structures of the IMPase protein may provide valuable clues for the development of inhibitors of IMPase. The bovine and human IMPase isoforms have been purified, crystallized and structures have been determined at resolutions of 1.4 Å (Gill *et al.*, 2005) and 2.1 Å (Bone *et al.*, 1992), respectively. However, in spite of many mouse IMPase-related studies and the benefits of mouse models in the development of therapeutic agents, a murine isoform has not yet been purified, nor has a crystal structure been obtained. The latter is necessary because although the enzyme is highly conserved, any significant differences between mouse and human IMPase might compromise the validity of mouse IMPase as a model in inhibition assays.

Here, we report the cloning, expression, purification and X-ray crystallographic structure of isoform 1 of murine IMPase and additionally of human IMPase solved at a higher resolution than previously reported.



2. Materials and methods

2.1. Cloning

The genes for mouse IMPase isoform 1 (*MmIMPase 1*) and the human orthologue (*HsIMPase 1*) were amplified from cDNA clones (IMAGE clones 6413389 and 3682657, respectively; Source Bioscience, Cambridge, England) by polymerase chain reaction (PCR; Saiki *et al.*, 1988) using the primer pairs (Sigma Genosys, Gillingham, England) shown in Table 1. The PCR products were digested with *NdeI* and *PstI* (NEB, Ipswich, Massachusetts, USA) and ligated into the corresponding sites of the pRSET5a expression vector (ampicillin resistance) using T4 DNA ligase (NEB) according to the manufacturer's instructions and transformed into *Escherichia coli* BLR (DE3) pLysS. Positive clones were selected on ampicillin agar and the inserted *impa1* gene sequences were verified by DNA sequencing (Geneservice, Oxford, England).

2.2. Expression and purification

The transformed BLR (DE3) pLysS cells were grown in LB broth containing 660 mM sorbitol and 2.5 mM betaine at 310 K until the OD₆₀₀ reached 0.9. Protein expression was then induced by the addition of 0.4 mM isopropyl β-D-1-thiogalactopyranoside (IPTG) and the culture was left overnight at 180 rev min⁻¹ and 303 K. Bacterial pellets were harvested by centrifugation at 1360g for 20 min at room temperature and resuspended in 100 ml buffer A (20 mM Tris-HCl, 1 mM EDTA pH 7.8) containing protease-inhibitor cocktail (Roche). The pellets were lysed by ultrasonication and the lysate was centrifuged at 30 000g for 30 min at 277 K. The supernatant was semi-purified by heating it to 345 K for 1 h as recommended by McAllister *et al.* (1992) and was centrifuged again at 30 000g for 30 min at 277 K. The supernatant was loaded onto a Q Sepharose anion-exchange column (GE Healthcare) pre-equilibrated with buffer A. The protein was eluted with an increasing concentration of buffer B (20 mM Tris-HCl, 1 mM EDTA, 1 M NaCl pH 7.8). Fractions were tested for phosphatase activity using inositol 1-phosphate as the substrate and malachite green reagent (Itaya & Ui, 1966). The active fractions were separated on a 10% SDS-PAGE reducing gel and fractions with the fewest contaminating bands were combined. The activity and purity were tested after each stage of chromatography and the active fractions with the least contamination were combined. The protein eluate was then subjected to a second stage of

Table 1

Primers for PCR amplification from mouse and human *impa1* cDNA.

NdeI (forward) and *PstI* (reverse) restriction sites are shown in bold.

IMAGE clone No.	Orientation	Sequence (5'-3')
6413389 (mouse)	Forward	AGGCATATGGCAGACCC TTGGCA
	Reverse	AGG CTGCAGT AAATCAGTCTAAATCAGTGAC
3682657 (human)	Forward	AATATTTTCAG CATATGGCTG ATCCTTG
	Reverse	ATGACTATGAG CTGCAGT AAATTAATCTTC

anion-exchange chromatography using a Mono Q column (GE Healthcare) and a gradient of buffers A and B. The purest most active fractions were again combined and loaded onto a Sephadex 75 column (GE Healthcare) for gel filtration using buffer A. The final eluate was concentrated to 7.5 mg ml⁻¹ using Amicon Ultra centrifugal filter units (10 kDa cutoff, Millipore). The protein concentration was calculated using the bicinchoninic acid method (Smith *et al.*, 1985) and the purity was verified using 10% SDS-PAGE.

2.3. Crystallization

Crystal screening was carried out using a Genesis Pro Team 150 robot (Tecan, Theale, England) and a Mosquito crystallization robot (TTP Labtech, Melbourn, England). Crystals were grown using the sitting-drop method.

Crystallization of *HsIMPase 1* was carried out in SWISSCI 3-well plates (catalogue No. 3W96TUVP) using 100 nl protein solution (10 mg ml⁻¹) at a 1:1 ratio with reagent. The reservoir well contained 40 μl reagent. The optimum conditions were 40% (w/v) PEG 3350, 0.2 M magnesium formate at room temperature.

Crystallization of recombinant *MmIMPase 1* was carried out in SWISSCI 2-well plates (catalogue No. MRC96TUVP) using 100 nl protein solution (7.5 mg ml⁻¹) at a 1:1 ratio with reagent. The reservoir well contained 50 μl reagent. The optimum crystals were obtained in conditions from the PACT screen: 0.2 M NaI, 20% (w/v) PEG 3350, 0.1 M bis-Tris propane pH 7.5 and pH 8.5 at 277 K.

2.4. Data collection and processing

Individual crystals were picked up using a nylon loop (Hampton Research, California, USA). They were briefly immersed in mother liquor containing cryoprotectant [33% (w/v) ethylene glycol for *MmIMPase 1* or 50% (w/v) glycerol for *HsIMPase 1*], flash-cooled at 100 K and stored in liquid nitrogen. For *MmIMPase 1*, data were collected to 2.4 Å resolution at 100 K on the I04-1 beamline at Diamond Light Source, Didcot, England using a Pilatus 2M detector (beam wavelength 0.980 Å, crystal dimensions 120 × 80 μm). For *HsIMPase 1*, data were collected to 1.7 Å resolution at 100 K at the European Synchrotron Radiation Facility (ESRF), Grenoble, France on an ADSC Q315r detector using 150 μm crystals (wavelength = 0.97625 Å).

The data were processed with *MOSFLM* (Battye *et al.*, 2011) and *SCALA* (Evans, 2006). Molecular replacement was carried out with *Phaser* (McCoy *et al.*, 2007) using the published structure of human IMPase (PDB entry 2hhm; Bone *et al.*, 1992) to determine the initial phases. The model was then subjected to multiple repeated rounds of model building in *Coot* (Emsley *et al.*, 2010) and refinement using *BUSTER* (Bricogne *et al.*, 2011).

3. Results and discussion

Mouse and human *impa1* were successfully cloned from cDNA into pRSET5a and overexpressed in *E. coli* BLR (DE3) pLysS. IMPase 1

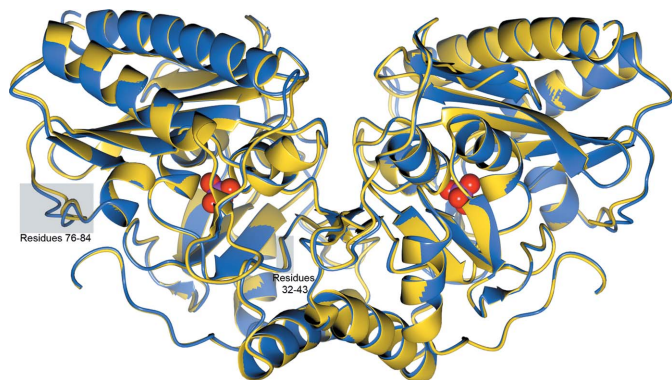


Figure 1
Overlay of *HsIMPase 1* (yellow) and *MmIMPase 1* (blue). Phosphate ions are shown in red as space-filling models. The two isoforms have 86.5% sequence identity and their core r.m.s.d. value was calculated to be 0.516 Å. Differences in the loops at the right and left edges of the overlaid structures are visible. The grey boxes highlight the subtle differences observed in two regions of the *HsIMPase 1* and *MmIMPase 1* structures.

Table 2X-ray data-collection and refinement statistics for *Mm*IMPase 1 and *Hs*IMPase 1.

Values in parentheses are for the highest resolution shell.

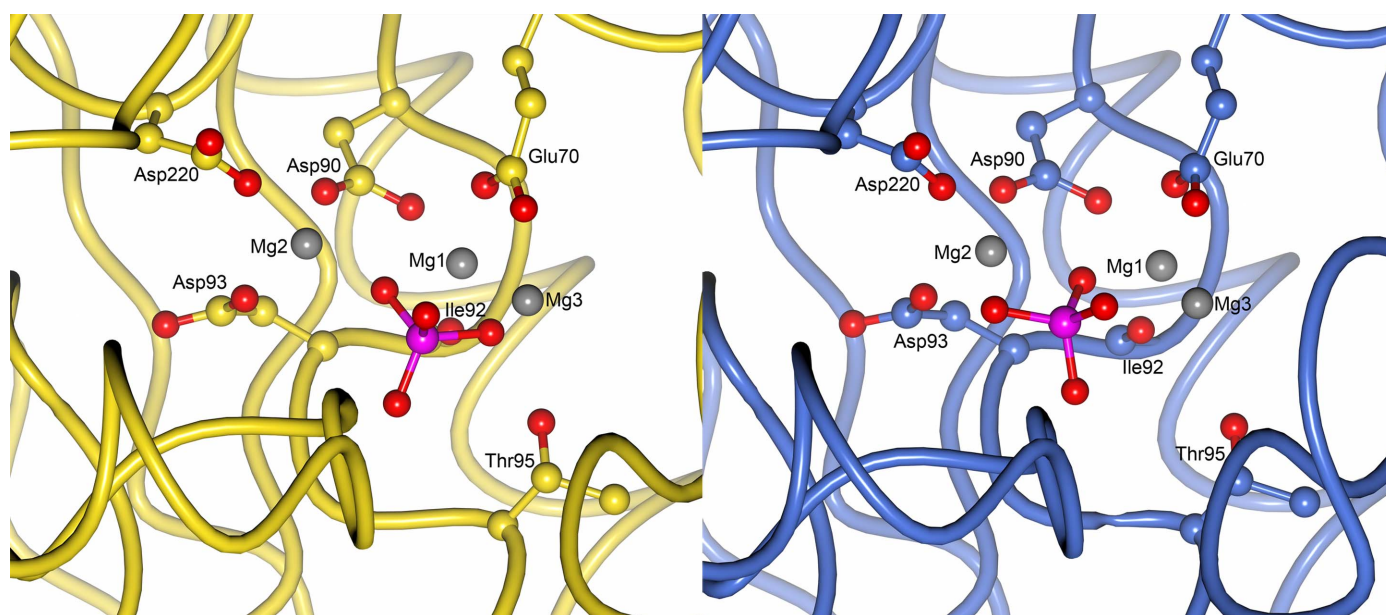
	<i>Mm</i> IMPase 1	<i>Hs</i> IMPase 1
Space group	$P2_1$	$P2_12_12_1$
Unit-cell parameters (Å, °)	$a = 86.78, b = 81.49,$ $c = 97.14, \beta = 133.7$	$a = 60.68, b = 76.05,$ $c = 118.09$
Temperature (K)	100	100
X-ray source	I04-1, Diamond Light Source	ID23-EH1, ESRF
Detector	Pilatus 2M	ADSC Q315r
Resolution (Å)	43.34–2.43 (2.56–2.43)	47.43–1.70 (1.79–1.70)
R_{merge} (%)	0.091 (0.503)	0.047 (0.442)
No. of unique reflections	46562 (6638)	60344 (8763)
Completeness (%)	98.8 (96.7)	99.3 (100.0)
Average multiplicity	6.3 (6.0)	4.7 (4.8)
$\langle I/\sigma(I) \rangle$	16.4 (3.2)	17.1 (3.5)
Refinement		
R_{work}	0.163	0.154
R_{free}	0.214	0.186
Mean B value (Å ²)	41.84	33.14
R.m.s.d. from ideal geometry		
Bond lengths (Å)	0.01	0.01
Bond angles (Å)	1.24	1.12
No. of refined atoms		
Protein	8377	4309
Heterogen	75	58
Solvent	848	596
Estimated coordinate error (Luzzati) (Å)	0.258	0.213
Ramachandran		
Favoured (%)	98.44	98.9
Allowed (%)	1.19	1.1

protein was purified using a combination of anion-exchange and gel-filtration chromatography and the purity was verified by SDS-PAGE. The molecular weight of each monomer was approximately 30 kDa and the proteins crystallized as dimers using the sitting-drop method. The *Mm*IMPase 1 crystals diffracted to 2.4 Å resolution and the *Hs*IMPase 1 crystals diffracted to 1.7 Å resolution; their overlaid structures are shown in Fig. 1. This is the first report of the structure of *Mm*IMPase 1 and the best resolution structure of *Hs*IMPase 1 obtained to date. The data-collection and refinement statistics are shown in Table 2.

Structurally, the two isoforms were found to be very similar and the core r.m.s.d. value was calculated to be 0.516 Å. The r.m.s.d. value for monomers *A* and *B* of *Mm*IMPase 1 was 0.283, while that for monomers *C* and *D* was 0.106. The core r.m.s.d. value for the published *Hs*IMPase 1 structure (Bone *et al.*, 1992; PDB 2hhm) and our *Hs*IMPase 1 structure was calculated as 0.346 Å and there was 100% sequence identity. The core r.m.s.d. value for 2hhm *versus* *Mm*IMPase 1 was found to be 0.636 Å with 86.4% sequence identity. The published bovine IMPase structure (Gill *et al.*, 2005; PDB entry 2bji) was also found to be similar. The only major difference observed between 2bji and *Hs*IMPase 1 and *Mm*IMPase 1 was the presence of a phosphate in the active site; this was not observed in the published bovine IMPase structure.

Some subtle differences in two loop-forming regions of the protein were observed between *Hs*IMPase 1 and *Mm*IMPase 1 (Fig. 1): primarily in the loop formed by residues 32–43 and additionally in the loop formed by residues 76–84. In the first loop residues 32 [Asn (human), Asp (mouse)], 35 [Leu (human), Ile (mouse)] and 40 [Val (human), Ala (mouse)] differed; although these are very minor differences, they are close to the active site. In the second loop (residues 76–84), residues 79 [Ser (human), Thr (mouse)], 80 [Ile (human), Val (mouse)], 81 [Leu (human), Phe (mouse)], 83 [Asp (human), Glu (mouse)] and 84 [Asn (human), Gln (mouse)] differed.

More significantly, the orientation of the phosphate group coordinated by the active-site residues was different in the two isoforms, as shown in Fig. 2. The different mode of binding in the two isoforms possibly leads to different magnesium coordination. The mouse isoform showed unidentate binding of all three magnesium ions to the phosphate ion. The human isoform, however, showed bidentate binding of two of the three magnesium ions to the phosphate ion. Since phosphate is one of the products of IMPase and is also a competitive inhibitor of the enzyme (Gee *et al.*, 1988), this may account for the differences in activity observed between the two isoforms. *Mm*IMPase 1 has an approximately fivefold lower specific activity than *Hs*IMPase 1. Additionally, the specific IMPase inhibitor L-690330 inhibits recombinant *Hs*IMPase 1 fivefold to tenfold more potently than mouse IMPase (from mouse brain homogenate; Attack

**Figure 2**

Structures showing the dissimilar orientation of the tetrahedral phosphate in *Mm*IMPase 1 (blue) and *Hs*IMPase 1 (yellow). The phosphate is shown coordinated by the amino-acid residues of the active site. Magnesium ions are shown as grey spheres and are labelled according to the coordination as suggested by Pollack *et al.* (1994).

et al., 1993). Although it is unlikely that higher resolution data will reveal significant differences in the *Mm*IMPase structure, they may reveal additional information about the solvent coordination in the active site, which could in turn illuminate the differences in activity between the human and mouse enzymes. This is the first report of *Mm*IMPase 1 and the best resolution structure of *Hs*IMPase 1 to be reported.

We thank Ralf Schoepfer for providing us with the pRSET5a vector, Robert Sim, Edith Sim and Ali Ryan for help with protein purification, Carmen Coxon and Parvinder Aley for help with preliminary experiments, Michael Field for proofreading and editing, and Elspeth Garman for her advice.

References

- Atack, J. R., Cook, S. M., Watt, A. P., Fletcher, S. R. & Ragan, C. I. (1993). *J. Neurochem.* **60**, 652–658.
- Battye, T. G. G., Kontogiannis, L., Johnson, O., Powell, H. R. & Leslie, A. G. W. (2011). *Acta Cryst.* **D67**, 271–281.
- Berridge, M. J. & Irvine, R. F. (1984). *Nature (London)*, **312**, 315–321.
- Bone, R., Springer, J. P. & Atack, J. R. (1992). *Proc. Natl Acad. Sci. USA*, **89**, 10031–10035.
- Bricogne, G., Blanc, E., Brandl, M., Flensburg, C., Keller, P., Paciorek, W., Roversi, P., Sharff, A., Smart, O. S., Vornrhein, C. & Womack, T. O. (2011). *BUSTER* v.2.10.0. Cambridge: Global Phasing Ltd.
- Chen, L. & Roberts, M. F. (1998). *Appl. Environ. Microbiol.* **64**, 2609–2615.
- Emsley, P., Lohkamp, B., Scott, W. G. & Cowtan, K. (2010). *Acta Cryst.* **D66**, 486–501.
- Evans, P. (2006). *Acta Cryst.* **D62**, 72–82.
- Gee, N. S., Ragan, C. I., Watling, K. J., Aspley, S., Jackson, R. G., Reid, G. G., Gani, D. & Shute, J. K. (1988). *Biochem. J.* **249**, 883–889.
- Gill, R., Mohammed, F., Badyal, R., Coates, L., Erskine, P., Thompson, D., Cooper, J., Gore, M. & Wood, S. (2005). *Acta Cryst.* **D61**, 545–555.
- Gillaspy, G. E., Keddie, J. S., Oda, K. & Gruijssem, W. (1995). *Plant Cell*, **7**, 2175–2185.
- Hallcher, L. M. & Sherman, W. R. (1980). *J. Biol. Chem.* **255**, 10896–10901.
- Itaya, K. & Ui, M. (1966). *Clin. Chim. Acta*, **14**, 361–366.
- McAllister, G., Whiting, P., Hammond, E. A., Knowles, M. R., Atack, J. R., Bailey, F. J., Maigetter, R. & Ragan, C. I. (1992). *Biochem. J.* **284**, 749–754.
- McCoy, A. J., Grosse-Kunstleve, R. W., Adams, P. D., Winn, M. D., Storoni, L. C. & Read, R. J. (2007). *J. Appl. Cryst.* **40**, 658–674.
- Pollack, S. J., Atack, J. R., Knowles, M. R., McAllister, G., Ragan, C. I., Baker, R., Fletcher, S. R., Iversen, L. L. & Broughton, H. B. (1994). *Proc. Natl Acad. Sci. USA*, **91**, 5766–5770.
- Saiki, R. K., Gelfand, D. H., Stoffel, S., Scharf, S. J., Higuchi, R., Horn, G. T., Mullis, K. B. & Erlich, H. A. (1988). *Science*, **239**, 487–491.
- Smith, P. K., Krohn, R. I., Hermanson, G. T., Mallia, A. K., Gartner, F. H., Provenzano, M. D., Fujimoto, E. K., Goeke, N. M., Olson, B. J. & Klenk, D. C. (1985). *Anal. Biochem.* **150**, 76–85.
- Takimoto, K., Okada, M., Matsuda, Y. & Nakagawa, H. (1985). *J. Biochem.* **98**, 363–370.